Mutants of the Cu_A Site in Cytochrome *c* Oxidase of *Rhodobacter sphaeroides*: I. Spectral and Functional Properties[†]

Yuejun Zhen,[‡,§] Bryan Schmidt,[‡] Uan Gen Kang,[‡] William Antholine,[||] and Shelagh Ferguson-Miller*[,‡]

Department of Biochemistry, Michigan State University, East Lansing, Michigan 48824, and National Biomedical ESR Center, Medical College of Wisconsin, Milwaukee, Wisconsin 53226

Received July 13, 2001; Revised Manuscript Received November 29, 2001

ABSTRACT: To study the functional significance of the unusual bimetallic Cu_A center of cytochrome *c* oxidase, the direct ligands of the Cu_A center in subunit II of the holoenzyme were mutated. Two of the mutant forms, M263L and H260N, exhibit major changes in activity (10% and 1% of wild-type, respectively) and in near-infrared and EPR spectra, but metal analysis shows that both mutants retain two coppers in the Cu_A center and both retain proton pumping activity. In M263L, multifrequency EPR studies indicate the coppers are still electronically coupled, while all the other metal centers in M263L appear unchanged, by visible, EPR, and FTIR spectroscopy. Nevertheless, heme a_3 is very slow to reduce with cytochrome *c* or dithionite under stopped-flow and steady-state conditions. This effect appears to be secondary to the change in redox equilibrium between Cu_A and heme *a*. The studies reported here and in Wang et al. [Wang, K., Geren, L., Zhen, Y., Ma, L., Ferguson-Miller, S., Durham, B., and Millett, F. (2002) *Biochemistry 41,* 2298−2304] demonstrate that altering the ligands of Cu_A can influence the rate and equilibrium of electron transfer between Cu_A and heme *a*, but that the native ligation state is not essential for proton pumping.

The structure, function, and spectral characteristics of the Cu_A center of cytochrome *c* oxidase (CcO)[1] have been the subject of intense controversy for many years (*1*). It is now clear that the unusual spectral characteristics of Cu_A are due to its dinuclear character, as initially concluded from spectral studies (*2*, *3*) and ultimately confirmed by high-resolution crystal structures of the holoenzyme (*4*−*8*) and the Cu_A domain (*9*, *10*). All the structures reveal two coppers bridged by two cysteines (Cys-252 and -256 in *Rhodobacter sphaeroides*), with two histidines (His-217 and -260) as the terminal ligands for each copper atom. A methionine (Met-263) ligates the more externally positioned copper through a relatively weak bond, while the other copper is even less strongly bound by the main chain carbonyl oxygen of a glutamate residue (Glu-254) (Figure 1). The structures of the holoenzyme reveal that Glu-254 is also a ligand of Mg through its side-chain carboxyl. The higher resolution structure of the Cu_A domain of *Thermus thermophilus* ba_3 oxidase (*10*, *11*) suggests that Glu-254, having a bond length of 2.6 Å,

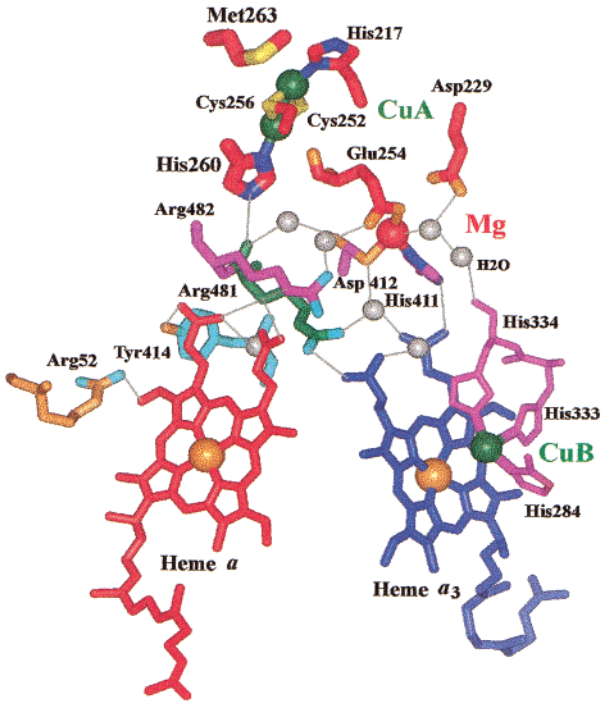

FIGURE 1: Structure and arrangement of the metal centers and associated amino acids in CcO. The amino acid side chains and two hemes are shown as sticks, with Cu_A, Cu_B, Mg, Fe, and water molecule as spheres. The thin lines indicate the location of hydrogen bonds. The figure was produced in InsightII from coordinates of *P. denitrificans* oxidase (1AR1) with the numbering of amino acid residues according to *R. sphaeroides* CcO.

[†] This work was supported by NIH Grant GM26916 (to S.F.M.) and NIH Grant RR01008 (to W.E.A.).

* To whom correspondence should be addressed. Phone: (517) 355-0199. Fax: (517) 353-9334. E-mail: fergus20@pilot.msu.edu.

[‡] Michigan State University.

[§] Current address: Myriad Genetic, Inc., 320 Wakara Way, Salt Lake City, UT 84108.

[||] Medical College of Wisconsin.

[1] Abbreviations: Ap, ampicillin; CCCP, carbonylcyanide-*m*-chlorophenylhydrazone; CcO, cytochrome *c* oxidase; *cox*II/*cox*III, genes encoding subunit II/subunit III of cytochrome *c* oxidase; DEAE, diethylaminoethyl; EDTA, ethylenediamine tetraacetic acid; EPR, electron paramagnetic resonance; FPLC, fast protein liquid chromatography; FTIR, Fourier transform infrared spectroscopy; HEPES, 4-(2-hydroxyethyl)-1-piperazineethanesulfonic acid; ICP, inductively coupled plasma emission spectroscopy; Kn, kanamycin; MCD, magnetic circular dichroism; NMR, nuclear magnetic resonance; N_2OR, nitrous oxide reductase; PCR, polymerase chain reaction; Sm, streptomycin; Sp, spectinomycin; Tc, tetracycline; TXFR, total-reflection X-ray fluorescence spectroscopy.

10.1021/bi0114628 CCC: $22.00
Published on Web 01/24/2002

should not be described as a direct ligand of the Cu_A center and that the two copper atoms are more asymmetric than previously indicated. However, there is some variability in the bond lengths determined for the various structures, and it remains to be seen whether these are due to the difference in resolution or to real differences in species or construct.

Time-resolved kinetic studies have shown that Cu_A is the initial electron acceptor from cytochrome *c* (*12*−*14*), followed by rapid transfer to heme *a* with a rate constant of 10^5 s^{-1} (*15*). According to Marcus theory (*16*), electron transfer in proteins is dependent on the driving force, the reorganization energy of the redox centers and the distance between them. Molecular orbital calculation (*17*, *18*) and paramagnetic NMR studies (*19*) demonstrate that the unpaired electron in the Cu_A center is delocalized in the Cu_2S_2 (Cys) structure, resulting in a lower reorganizational energy and contributing to the rapid electron transfer from cytochrome *c* to heme *a* (*20*).

Among the various factors influencing the electron-transfer rate, the role of the intervening medium between the redox centers is most controversial (*21*, *22*). In bovine CcO, Cu_A is 19 Å (metal-to-metal) from heme *a* and 22 Å from heme a_3 (*4*). The almost equal distance from Cu_A to the two heme groups, together with the fact that the electron-transfer rate from Cu_A to heme *a* appears much faster than to heme a_3, leads to the question of whether there are special features of the Cu_A center, or the intervening protein structure, that contribute to the apparent selectivity for transferring electrons to heme *a*. The smaller reorganization energy associated with electron transfer between Cu_A and heme *a* has been suggested to account for the difference (*20*), but a possible through-bond electron-transfer pathway from Cu_A to heme *a* has also been invoked (*23*). The suggested route involves one of the Cu_A ligands, His-260, the peptide bond between an arginine pair immediately below it, and several hydrogen bonds connecting these regions to a heme *a* propionic acid substituent (*6*, *23*) (Figure 1).

In this study, the operon encoding subunit II and subunit III (*cox*II/III) was deleted from the *R. sphaeroides* chromosome and the strain was complemented with a plasmid containing the entire *cox*II/III operon (see Supporting Information), making it possible to use site-directed mutagenesis techniques to study the structure and functions associated with subunit II in the holoenzyme (*24*) and to address questions regarding rapid electron transfer to heme *a* and coupled proton translocation in CcO.

METHODS AND MATERIALS

Material. All restriction endonucleases, other DNA-modifying enzymes, and the DIG/Genius system were from Boehringer Mannheim (Indianapolis, IN); plasmids pHP45Ω, pRK415-1 and *Escherichia coli* strain S-17-1 were obtained from the sources indicated in Shapleigh and Gennis (*25*). Plasmid pYJ100 containing *cox*II and *cox*III was originally prepared by Cao et al. (*26*). pJP5603 (Kn^R) was obtained from Dr. Gennis at the University of Illinois.

Cell Growth. E. coli strain S-17-1 and TG1 were grown in LB medium at 37 °C. Plasmids pUC19, pRK415-1, and pJP5603 and their derivatives were maintained in the presence of the following antibiotics: ampicillin (Ap) (50 μg/mL), tetracycline (Tc) (15 μg/mL), and kanamycin (Kn) (25 μg/mL), respectively.

R. sphaeroides strain Ga was grown aerobically in Sistrom's media at 30 °C with rapid swirling. Strains of *R. sphaeroides* harboring a streptomycin/spectinomycin (Sm/Sp) resistance cartridge were grown in the presence of streptomycin (Sm) (50 μg/mL) and spectinomycin (Sp) (50 μg/mL). For cells containing pRK415-1 derivatives, Tc was added to the medium at 1 μg/mL.

Site-Directed Mutagenesis. The mutants were designed using the systems described in detail in Zhen (*27*). Briefly, a 500−600 bp fragment of *cox*II containing the residue to be mutated was amplified using the overlap extension PCR method (*28*), with the desired mutations in the primers. The final PCR products were sequenced to confirm the presence of the desired mutation before ligating back into the *cox*II/III operon in pYJ100.

In a similar approach, a "loop" mutant (LpM) was created by replacing the Cu_A-binding loop, **Cys**-Ser-**Glu**-Ile-**Cys**-Gly-Ile-Ser-**His**-Ala-Tyr-**Met**-Pro-Ile, residue numbers 252−265 of subunit II, with a sequence of **Cys**-Ser-Glu-Pro-Gly-**His**-Ser-Ala-Leu-**Met**-Lys-Gly from azurin, in an attempt to convent the dinuclear Cu_A center to a blue copper center.

Protein Expression and Purification. All the mutants were expressed using the expression vector pRK415-1, after conjugating it with the subunit II deletion strain YZ200. H260N, M263L, and LpM were also overexpressed using the system described in Zhen et al. (*29*) and purified using metal-affinity chromatography and additional purification by DEAE-FPLC chromatography (*29*).

Spectrophotometric Analysis. Optical spectra were recorded as described in ref *29*, and the CO-difference spectra were done as described in ref *24*.

Activity Assay. The turnover numbers of the purified oxidases were measured polarographically at 30 μM cytochrome *c* as described in ref *30*.

Metal Assay. Metal analyses were done using inductively coupled plasma emission (ICP) spectroscopy at the chemical analysis laboratory at the University of Georgia and total-reflection X-ray fluorescence spectrometry (TXRF) at the physics department of the University of Göteborg, Sweden. The sample concentrations were in the range of 30−70 μM.

EPR Spectroscopy. Measurements were performed for the purified oxidase in a solution of 10 mM Tris-HCl, 40 mM KCl, pH 8.0, 0.1% lauryl maltoside. The sample preparations for high Mg or high Mn content oxidases were the same as described in ref *31*. Multifrequency measurements were made using loop-gap resonators and low-frequency microwave bridges designed and built at the National Biomedical ESR Center (Medical College of Wisconsin, Milwaukee, WI) (*32*, *33*). X-band spectra were obtained on a Varian Century Series spectrometer at Milwaukee and on a Bruker ESP-300E spectrometer at Michigan State University.

FTIR Spectroscopy. FTIR spectra were recorded for the purified oxidases after the enzymes were first made anaerobic by repeated cycles of vacuum and CO flushing in small vials, and then sodium dithionite was added to a final concentration of 30 mM. The sodium dithionite solution had been made anaerobic with CO gas. Wild-type oxidase was incubated for 1 h before being transferred to the CaF_2 windows, while M263L and H260N were incubated for 6−8 h for completed reduction. Instrumentation and experimental conditions were as described in the figure legends.

Heme a and a_3 Reduction Assay. The reduction of heme *a* and a_3 was done anaerobically with an OLIS-RSM-1000 stopped-flow spectrometer by rapidly mixing 5 μM CcO and 30 mM sodium dithionite in 200 mM Bis-Tris-propane, pH 6.5, 0.1% LM. Both the oxidase and the dithionite solutions were degassed under oxygen-free nitrogen for at least 15 min before being transferred to the stopped-flow instrument equipped with anaerobic tonometers. The reduction of oxidase was followed by rapid scanning, 1000 scans/s from 390 to 620 nm. At least three data sets were recorded and averaged. The data of the reduced-minus-oxidized difference spectra were analyzed using global fitting software provided with the OLIS-RSM-1000 stopped-flow spectrometer. The first-order rate constants for kinetically independent species, heme *a* and a_3, were determined.

Proton Pumping Assay. Cytochrome oxidase vesicles were made by the cholate dialysis method (*34*), with 20 mg/mL asolectin lipids and 2 μM oxidase. Proton pumping activity was measured with an OLIS-RSM-1000 stopped-flow spectrometer as described in ref *35*, in a solution of 50 μM HEPES−KOH, 45 mM KCl, 44 mM sucrose, 1 mM EDTA, with one syringe containing 200 μM Phenol Red and 16 μM prereduced cytochrome *c*, and the other one with 0.5 μM oxidase in vesicles. One thousand scans per second were recorded from 500 to 650 nm. At least three data sets were averaged to give the data shown.

RESULTS

Mutagenesis of the Cu_A Center. (i) Expression of Mutants in Rhodobacter Membranes. To study the significance of the dinuclear character of Cu_A, a number of mutants were created, including H217C, H217G, C256S, H260C, H260G, H260N, M263L, and LpM, with the aim of altering the Cu_A center to different degrees.

All the mutated oxidases were expressed at reasonable levels, in contrast to attempts to make similar mutations in yeast (*36*), but the levels of some were decreased to less than 50% that of wild-type (data not shown). With mutated oxidases of low activity there is considerable selective pressure to eliminate the part of the plasmid containing the *cox*II/III gene, contributing to lower oxidase expression. Structural instability, as suggested by the blue-shifted heme *a* α-peaks in H217G, C256S, and H260G (data not shown), can also contribute to low apparent expression. However, despite their low activity, expression of H260N and M263L mutant forms was close to wild-type when grown fresh from newly conjugated cells, and expression was further increased using the overexpression system described in Zhen et al. (*29*). We have focused on the characterization of these two mutants, due to their availability in sufficient amounts and their representative properties, one mildly (M263L) and one greatly (H260N) disrupted in the spectral properties of their Cu_A centers. Similar mutational analyses have been done in the *P. denitrificans* holoenzyme and Cu_A domain (*37*−*40*). However, new aspects of activity are measured in the *Rhodobacter* CcO mutants, and different conclusions are drawn on the effects of similar mutations (see below).

(ii) Attempted Chemical Rescue of H217G and H260G. H217G and H260G, in which the histidines are replaced with glycine, are presumably left with cavities inside the protein where the imidazole side chain was. Chemical rescue with imidazole (*41*, *42*) was tried by growing the mutant *R. sphaeroides* strains in the presence of imidazole. However, the cell growth was severely inhibited by 10 mM imidazole, the concentration used successfully in *E. coli* (*41*). Failure to rescue His-to-Gly mutants during growth was previously observed in *R. sphaeroides* (*43*), suggesting that *R. sphaeroides* may not have the transport system to take up imidazole, or takes it up too well, to the detriment of cell growth.

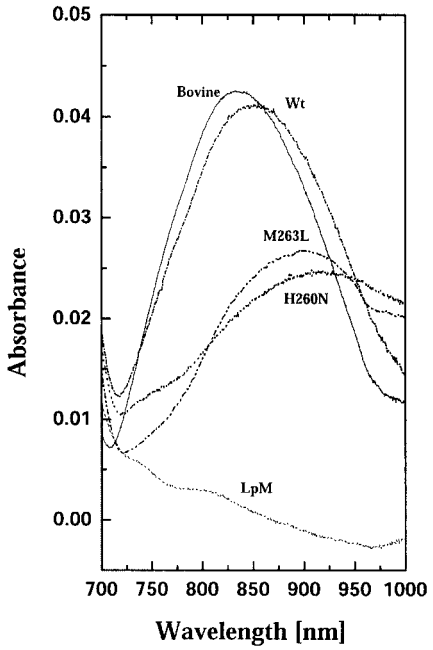

FIGURE 2: Near-infrared spectra of bovine and *R. sphaeroides* CcO. Oxidized-minus-reduced spectra for bovine, wild-type and mutated *R. sphaeroides* CcO are shown. The spectra were recorded as described in Zhen et al. (*24*). All the samples are scaled to the same concentration of 20 μM.

(iii) Loop Mutant (LpM). The purified LpM, designed to create a blue-copper center, has a shifted heme spectrum, with the α and Soret peaks centered at 600 and 440 nm, respectively. EPR analysis of this mutant shows that the Cu_A signal is completely gone, but the characteristics of a type 1 copper EPR signal are not present either (data not shown), indicating that the attempt to convert the Cu_A center to a type 1 copper did not succeed. Without the Cu_A center, the 830 nm absorption peak from Cu_A is not present (Figure 2), and the purified oxidase has no measurable activity.

Characterization of H260N and M263L. (i) O_2 Consumption Activity. The activities of these two mutants are very low, about 1% and 10% of wild-type activity for H260N and M263L, respectively (Table 1). The residual activity measured for H260N is not due to any exogenous contaminant since it is reproducible in repeated preparations and purifications, and can be inhibited by cyanide.

(ii) Optical Spectra. The reduced spectrum of M263L is almost identical to that of wild-type (Table 1), indicating that the mutation has no effect on the structures of the two heme groups on subunit I. The α-peak of the reduced spectrum for H260N is blue-shifted about 1 nm, indicating slight structural disturbance of the heme *a* center; however, its Soret/α -peak ratio is the same as that of wild-type, indicating no differential loss of heme *a* or a_3.

The CO-binding abilities of the mutants are also similar to that of wild-type (Table 1) (*30*), indicating that the heme a_3−Cu_B center is not disturbed structurally.

Table 1: Characteristics of *R. Sphaeroides* Cytochrome *c* Oxidase Subunit II Mutants H260N and M263L

enzyme	optical spectra		$\epsilon_{(830)}$	turnover	Cu/Fe ratio		CO-binding[a]	EPR spectra	
	α-peak	Soret/α	(cm^{-1} mM^{-1})	(s^{-1})	ICP	TXRF	(%)	Cu_A	Mn
wild-type	606	5.6 ± 0.1	2.06 ± 0.05	1700 ± 200	1.51 ± 0.08	1.26 ± 0.08	100	normal	normal
H260N	605	5.5 ± 0.1	1.34 ± 0.03	15 ± 10	1.49 ± 0.05	1.22 ± 0.06	96	distorted	distorted
M263L	606	5.6 ± 0.1	1.23 ± 0.03	150 ± 50	1.49 ± 0.05	1.17 ± 0.04	95	distorted	normal

[a] Spectral determination as described in Zhen et al. (*24*). Error on measurements is ±10%.

Oxidized CcO has a weak absorption in the near-infrared region which has been assigned to Cu_A (*44*). In bovine CcO, this band is centered at 830 nm (Figure 2). *R. sphaeroides* CcO also absorbs in the near-infrared region with a similar extinction coefficient of 2.0 cm^{-1} mM^{-1} for the oxidized minus reduced spectra (Figure 2); however, the peak of the absorption for *R. sphaeroides* CcO is at 850 nm, indicating it is not identical to bovine CcO.

This 850 nm band in the oxidized enzyme is shifted and diminished in both H260N and M263L, with a decreased apparent oxidized minus reduced extinction coefficient of 1.34 and 1.23 $cm^{-1}mM^{-1}$, respectively (Table 1) (Figure 2).

(iii) FTIR Spectra. Fourier transform infrared (FTIR) spectra provide additional information about the heme a_3-Cu_B center by measuring the stretching frequency of the C−O bond, which is sensitive to the local environment of the center (*45*). In reduced CcO at low temperatures, CO will bind to heme a_3 in the dark, and Cu_B after a light flash. The C−O stretching frequency is influenced by the metal center to which it is bound and the environment around it, providing one of the few assays for the integrity of the Cu_B site.

The FTIR difference spectra of wild-type, M263L, and H260N are shown in Figure 3. In the wild-type spectrum, two negative peaks associated with the Fe_{a3}-bound CO are observed at 1953 and 1966 cm^{-1}, respectively, designated as α- and *β*-forms (*46*). The frequencies of the two peaks for Fe−CO in wild-type are similar to those observed previously (*45*, *46*), but only one positive Cu_B-CO peak is resolved at 2060 cm^{-1}, corresponding to the α form. For M263L and H260N, the frequencies of Fe−C−O and Cu−C−O and the relative ratios of the α- and *β*-forms are the same as wild-type, confirming unaltered heme a_3 and Cu_B centers.

(iv) Metal Analysis. Metal analyses were done on wild-type and mutants using both ICP and TXRF spectroscopies (Table 1). The Cu-to-Fe ratio found for wild-type CcO from ICP analysis is 1.51, which is in good agreement with the known three Cu and two Fe atoms per CcO molecule. The Cu/Fe ratio measured by TXRF for wild-type oxidase is slightly lower than the theoretical number. For H260N and M263L, their Cu/Fe ratios are comparable to that of wild-type oxidase using either method, indicating that these two mutants both retain two coppers at the Cu_A site.

(v) EPR Analysis of Cu_A and Hemes. In wild-type *R. sphaeroides* CcO, the EPR signals at $g = 2.83$, 2.31, and 1.62 arise from the low spin heme *a*, and those at $g = 2.19$ and 2.00 from Cu_A (*30*) (Figure 4). Due to antiferromagnetic coupling, the high spin heme a_3 and Cu_B are normally EPR-silent. In M263L, the heme *a* signal at 2.83 is identical to wild-type; in H260N, the signal is shifted to $g = 2.85$, indicating some slight alteration in the region of heme *a*. The spectra of H260N and M263L both reveal significant changes in the Cu_A centers compared to wild-type. In the $g_\perp$ high field region, partial hyperfine splitting was resolved in the spectrum of M263L. In the g_{II} lower field region, the single peak at $g = 2.19$ in the wild-type is gone, replaced by some hyperfine splittings in M263L. These results agree with observations on a similar mutant created in *P. denitrificans* (*47*). For H260N, the alteration of the Cu_A center is even more dramatic, but no apparent hyperfine splitting pattern is present.

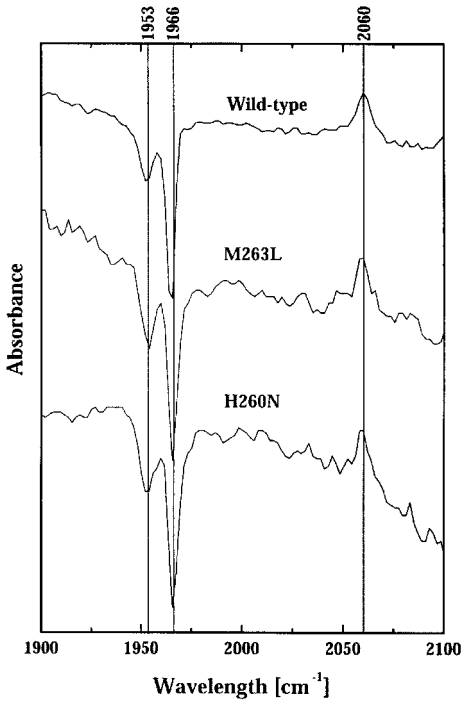

FIGURE 3: FTIR absorbance spectra (light-minus-dark) of wild-type oxidase, H260N, and M263L from *R. sphaeroides*. The "light-minus-dark" FTIR spectrum reveals the distinct C−O stretching frequencies associated with the $Fe_{a3}-C-O$ and Cu_B-C-O forms as negative and positive peaks, respectively. The Fe−CO absorption bands in wild-type and mutant oxidases are centered at 1953 cm^{-1}, and 1966 cm^{-1}, while the Cu−CO is at 2060 cm^{-1} For photodissociation of CO from heme a_3, the samples were illuminated with a 150 W halogen bulb. The infrared component of the actinic light of a 150 W halogen bulb was removed by filters. The spectra were recorded at 200 K on a Nicolet 740 spectrometer with a KBr beamsplitter and a Graseby mercury−cadmium-telluride (MCT). The double-sided interferograms were collected at 4 cm^{-1} resolution and apodized by using a Happ-Ganzel apodization function. The temperature was controlled by a Lake Shore Cryogenic temperature control unit (Model 321). An oxidase concentration of about 200 μM in 100 mM KH_2PO_4 buffer, pH 7.0, with 0.2% LM was used.

A more detailed analysis was carried out with multifrequency EPR, since in wild-type oxidase the theoretical seven-line hyperfine pattern characteristic of a mixed-valence Cu_A center (*48*) is not resolved at X-band frequency, but can be better resolved at C- and S-band frequencies to compare with the mutant forms.

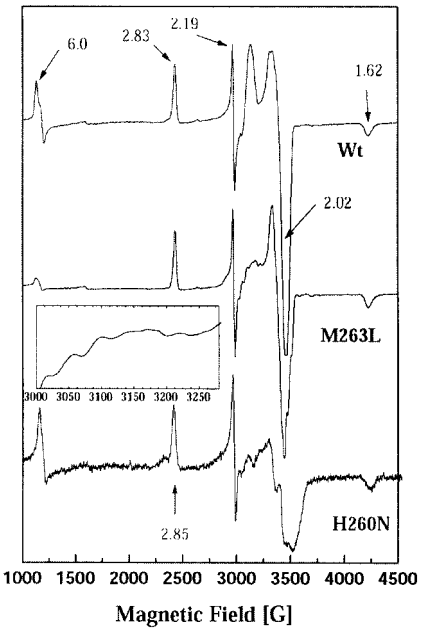

FIGURE 4: X-band EPR spectra of wild-type oxidase, H260N, and M263L. The spectra were recorded at 100 K using a Bruker ESP-300E spectrometer. The related *g* values are indicated in the plots. The rhombic signal with *g* values of 2.83, 2.31, and 1.62 is from the low-spin heme *a*, whereas the $g = 6.0$ signal arises from a small amount of uncoupled high-spin heme a_3. The axial signal with *g* values of 2.19 and 2.02 are from the Cu_A center. The *inset* is the enlarged g_{II} region for M263L from 3000 to 3300 G. Spectrometer conditions: microwave frequency 9.48 GHz; microwave power 2 mW; modulation amplitude 12.7 G. Temperature was maintained at 10 K using an Oxford helium cryostat assembly (Oxford Instruments, Concord, MA).

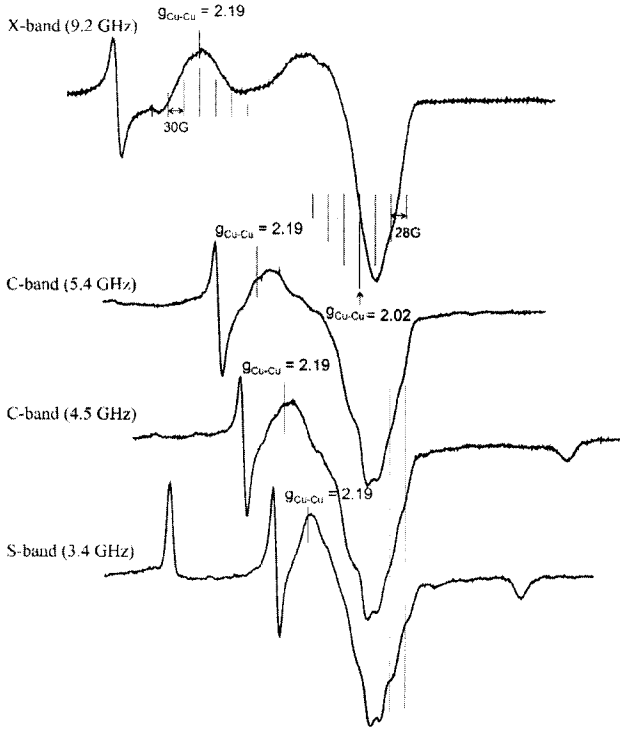

FIGURE 5: Mutifrequency EPR spectra for wild-type *R. sphaeroides* CcO. The microwave frequencies used in the experiments are S-band (3.4 GHz); C-band (4.5 and 5.4 GHz); X-band (9.2 GHz). Temperatures of 15 K were maintained with a helium flow system (Air Products, Allentown). Spectrometer conditions: modulation amplitude 5 G, microwave power 25 dB with an incident power of 10 mW.

For wild-type *R. sphaeroides* CcO, the different frequency EPR spectra are compared in Figure 5. In the X-band spectrum, a single peak at $g = 2.19$ is seen in the low field region and one at $g = 2.02$ in the high field region. At C- and S-band, lines from a seven-line hyperfine pattern begin to be resolved, from which a splitting constant can be determined, $A_X^{Cu} = 28$ G (Table 2). The splitting constant for A_Z^{Cu} is about 30 G as determined from the line width of the line in the g_{II} region (Figure 6), but the hyperfine structure is not resolved. The EPR parameters of the bovine CcO and the nitrous oxide reductase (N_2OR) Cu_A sites are not identical to the *R. sphaeroides* CcO, indicating some subtle structural difference, consistent with the near-infrared spectra (Figure 2).

Multifrequency EPR spectra were also obtained for M263L (Figure 6). Hyperfine lines were well resolved, even at X-band, in the high field $g_\perp$ region. A copper splitting A_X^{Cu} of 36 G can be measured. To determine whether these high field lines are from a seven-line pattern, i.e., a mixed valence dinuclear copper site, or a four-line pattern, a distorted type 1 site (*37*, *38*), *g*-values were calculated as a function of microwave frequency assuming a seven-line pattern or a four-line pattern (Table 3). Since the *g*-value was found to be invariant for a seven-line pattern and not for a four-line pattern, we conclude that the altered Cu_A site in M263L is still a mixed valence dinuclear site with $g_{Cu-Cu} = 2.02$.

In the g_{II} region, hyperfine lines were resolved in the X-band spectrum of M263L, while the intensity of the pattern is noticeably less than for the wild-type. Assuming that the reduction of the intensity is due to inequivalent couplings from the two coppers in the mixed valence site resulting in inhomogeneous line-broadening, a *g*-value of 2.17, an A_{Z1}^{Cu} value of 65 G and an A_{Z2}^{Cu} value of 58 G account for the lines resolved in the X-band spectra (Figure 6). The lines are better resolved at the edge of the pattern where there are fewer transitions and less resolved in the center where there are more transitions. In fact there likely exists a range of values due to an increase in *g*- and *A*-strain that results in the decreased intensity in the g_{II} region. The resolved lines are a subset of all the orientations in the axial direction and vary somewhat from sample to sample (Figures 4 and 6). The strain is much less in the $g_\perp$ region where the lines are resolved and the intensity is not changed at all microwave frequencies for all M263L samples. The mutation of the methionine ligand in M263L likely changes the equivalency of the two copper atoms and slightly alters their electronic structures, but the effect is not severe enough to decouple the two copper atoms, in agreement with conclusions from studies of the Cu_A domain of the ba_3 oxidase (*11*).

For H260N, the alteration of the Cu_A center is even more dramatic (Figure 4), in contrast to studies of an equivalent mutation in the engineered Cu_A domain in azurin (*49*).

Table 2: Mutifrequency EPR Parameters for Mixed-Valence Cu_A Sites

sample	g_z^{Cu-Cu}	g_x^{Cu-Cu}	A_Z^{Cu} (G)	A_X^{Cu} (G)	ref
R. sphaeroides (wt)	2.19	2.02	30	28	this work
Bovine	2.18	2.00	38	23	Antholine et al.
N_2OR	2.18	2.02	38	28	Antholine et al.
M263L	2.19	2.02	65; 57	36	this work

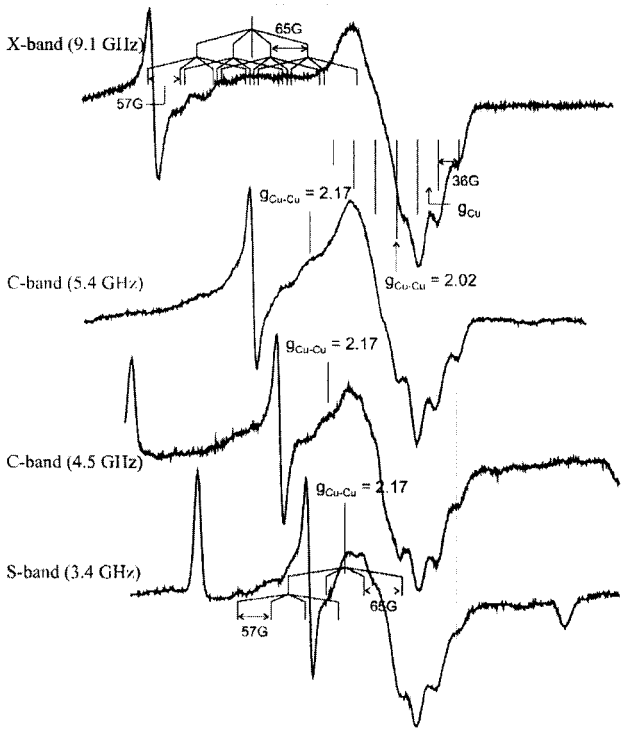

FIGURE 6: Mutifrequency EPR spectra for M263L. The microwave frequencies used in the experiments are S-band (3.4 GHz); C-band (4.5 and 5.4 GHz); X-band (9.2 GHz). Temperatures of 15 K were maintained with a helium flow system (Air Products, Allentown). Spectrometer conditions were as described in Figure 6.

Table 3: Mutifrequency EPR Parameters for M263

microwave frequency	g_{Cu-Cu}[a]	g_{Cu}[a]	A_x^{Cu-Cu} (G)
X-band (9.2 GHz)	2.02	1.99	35
C-band (5.4 GHz)	2.02	1.97	37
C-band (4.5 GHz)	2.02	1.96	36
S-band (3.3 GHz)	2.02	1.94	36

[a] g_{Cu-Cu} calculated assuming the resolved lines on the high field side of the spectrum arise from a 7-line pattern and g_{Cu} from a 4-line pattern.

However, no apparent hyperfine splitting pattern was present in the X-band spectrum, leaving its electronic structure unresolved.

(vi) EPR Analysis of the Mn Center. In *R. sphaeroides* CcO, it has been shown that the Mg atom located at the interface of subunit I and II can be replaced by a Mn atom when the cells are grown in a higher than normal ratio of Mn to Mg (*31*). The distinct EPR spectrum of Mn can then be used as a probe to check the structural integrity of the interface. The Mn EPR spectra were recorded for wild-type and the two mutants (*50*). While the Mn EPR spectrum of H260N was altered as compared to that of the wild-type CcO, suggesting some delocalized effect of the mutation, M263L did not show any changes, indicating a strictly localized effect of the mutation.

(vii) Heme a and a_3 Reduction Kinetics. Heme a_3 in M263L and H260N was difficult to be reduced with dithionite, as indicated by the persistence of a 418 nm peak, while heme a_3 of wild-type CcO was quickly reduced (Figure 7A). To investigate this unexpected phenomenon, M263L was mixed anaerobically with dithionite as the reducing agent in a stopped-flow apparatus. As shown in Figure 7B, after 14 s, the absorbance of 606 nm reaches almost the same

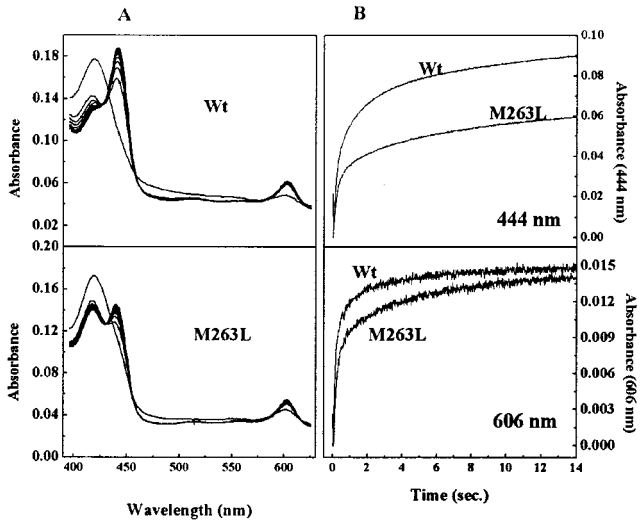

FIGURE 7: Heme *a* and a_3 reduction assay in wild-type oxidase and M263L. The experiments were done in a stopped-flow apparatus in a solution of 100 mM Bis-tris-propane, pH 6.5, 0.1% LM, with 2.5 μM oxidase and 15 mM dithionite. (A) The spectral change for wild-type (top) and M263L (bottom) in the visible region for the first 5 s of dithionite reduction. (B) The kinetic of the reduction of heme *a* and a_3 followed at the Soret (top) and α-peak (bottom).

levels as that of the wild-type oxidase, but the absorbance change at 444 nm for M263L is much smaller than that of the wild-type. In CcO, previous studies have shown that heme *a* contributes most (~80%) of the 606 nm absorbance, but only 50% of the 444 nm absorbance. The results suggest that heme *a* was completely reduced within the first 14 s, while the reduction of heme a_3 in M263L is slow. However, when reduction rates for heme *a* and a_3 were analyzed using a global fitting program, the observed rates of reduction in M263L were 3.9 (±0.2) s^{-1} and 0.14 (±0.01) s^{-1}, respectively, for heme *a* and a_3, both about 50% lower than those observed for wild-type CcO, 7.6 (±0.9) s^{-1} and 0.31 (±0.01) s^{-1}. Thus, the lesser level of a_3 reduction must reflect a change in the equilibrium, not in relative rate of electron transfer to heme a_3.

(viii) Proton Translocation. The proton pumping activity of purified wild-type and mutant oxidases reconstituted into phospholipid vesicles was measured by a stopped-flow scanning spectrophotometer (*35*, *50*).

In the presence of valinomycin, an ionophore that abolishes the membrane potential, the addition of reduced horse cytochrome *c* results in rapid acidification outside the vesicles (Figure 8), indicating proton pumping by wild-type CcO. When proton uncoupler CCCP is added, a large alkalinization is observed, due to rapid equilibrium of protons across the lipid bilayer to support water formation in the interior of the vesicles. The proton pumping stoichiometry (H^+/e^-) for wild-type oxidase is about 1 (±0.2). Both M263L and H260N show proton pumping activity with stoichiometries of 0.9 (±0.2) H^+/e^- and 0.3 (±0.1) H^+/e^-, respectively.

DISCUSSION

The 830 nm Band of the CuA Center. Despite considerable evidence for the correlation of the 830 nm band intensity with the redox state of Cu_A (*51*−*54*), various studies have suggested that the two heme groups (*55*) and Cu_B (*56*) might also contribute to the absorbance in this region, and Hendler

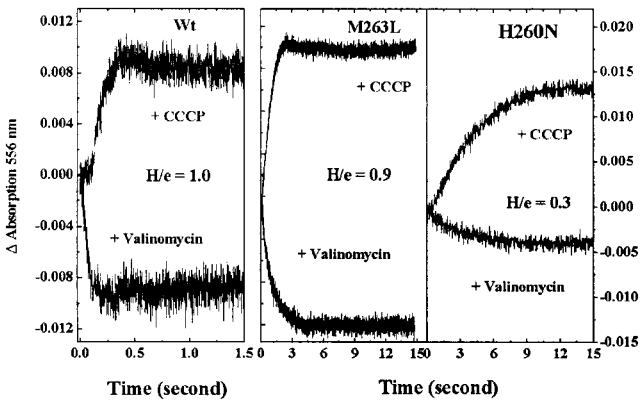

FIGURE 8: Proton pumping assays for wild-type, M263L, and H260N oxidases. The proton pumping activities were measured by following phenol red absorbance changes with oxidase vesicle in a stopped-flow apparatus as described in the Materials and Methods. The spectra show increased absorbance for alkalinization and decreased absorbance for acidification under uncoupled conditions. The spectra were corrected for back leak. The H^+/e^- ratios were calculated from the amplitudes of the acidification and alkalinization. The absorbance scale on the left refers to the wild-type measurement; the absorbance scale on the right refers to both mutant measurements.

(*57*) cautions that the 830 nm absorbance cannot be used as a indicator of the redox state change of Cu_A center.

The independent expression of the soluble Cu_A domain of CcO removes any heme spectral contributions; this construct retains the broad absorbance in the 830 nm region, showing that Cu_A is the major contributor to this absorbance. However, the absolute extinction coefficient of the 830 nm band for the oxidized Cu_A center in the soluble domain [1.6 mM^{-1} cm^{-1} (*58*)] is considerably smaller than that of the holoenzyme (3.2 cm^{-1} mM^{-1}), indicating that other metal centers could contribute to the absolute absorbance in this region.

The 830 nm band is only present in the oxidized enzyme; upon reduction, the band disappears and small absorbance bands appear in the region of 700 to 800 nm, which have been assigned to heme *a* and a_3 (*59*, *60*). Although no major absorbance peak is resolved in the 830 nm region in the reduced spectrum, the baseline absorbance is quite high, which results in a smaller oxidized-minus-reduced difference extinction coefficient (2.06 cm^{-1} mM^{-1}).

In this study, a mutated oxidase (LpM) was created, which has completely lost the Cu_A center and the 830 nm band in the oxidized spectrum, but retains a relatively normal a/a_3 ratio. Upon reduction, only a small baseline change is observed, supporting the essentially exclusive role of Cu_A in the redox changes at 830−850 nm. Optical and MCD spectra of the aa_3-600-type quinol oxidase also show that the 830 nm absorbance is not present (*61*).

EPR studies have shown that the electronic structure of the Cu_A sites in bovine and *R. sphaeroides* are slightly different (*30*) (Table 2). In addition, the near-infrared spectrum of oxidized *R. sphaeroides* CcO is at 850 nm, rather than at 830 nm as in bovine CcO. These results point to some unique aspects of the structure of the two copper atoms of the bovine and bacterial Cu_A centers, although crystal structures of these two enzymes are not yet at sufficiently high resolution to reveal the nature of the differences.

The correlation of the missing of Cu_A site in LpM with no cytochrome *c* oxidase activity for this mutant also strongly supports the conclusion that the Cu_A center in CcO is the only site that can accept electrons from cytochrome *c*.

Effects of H260N and M263L Mutations on Spectral Characteristics of CcO. (i) Visible, EPR, FTIR Analysis of Heme a, a_3, and Cu_B. Visible spectral analysis shows that the heme *a* center is intact in M263L with an α-band at 606 nm. The heme a_3-Cu_B center in M263L is also not disturbed, as probed using FTIR spectroscopy and CO-binding. The internal electron-transfer events in M263L have been investigated using the flash photolysis technique (*62*). In the mixed-valence enzyme, the reverse electron-transfer rate from heme a_3 to heme *a* in M263Lwas the same as in wild-type, which further confirmed that heme *a* and a_3 were not altered. The Mg center, although sharing a ligand with Cu_A, has a normal EPR spectrum when substituted with Mn. So the mutation of M263L has no detectable global effect on the protein structure and the changes observed in activity of the mutant can be attributed to the localized effects on the Cu_A center.

A similar mutant, M227I, was created in the oxidase from *P. denitrificans* (*37*), in which the equivalent residue to Met-263 was mutated to isoleucine. Unlike the *R. sphaeroides* M263L, the CO difference spectra of M227I retained a strong 417 nm peak, interpreted as being due to an alteration of heme a_3 in M227I. However, it is more likely that the altered CO-binding spectrum of M227I is due to an indirect effect on the reducibility of heme a_3 as a result of the altered equilibrium between Cu_A and heme *a* (Figure 7) (*62*).

The mutation in H260N causes more disturbance of the oxidase, as evidenced by the shift of the heme *a* optical (605 nm) and EPR ($g = 2.85$) spectra and the alteration in the Mn EPR spectrum. The crystal structures of CcO reveal that there is an extended hydrogen-bonded network including a number of waters at the interface between subunits I and II (*63*) (Figure 1), in which His-260 plays a role. This Cu_A ligand is hydrogen-bonded to the peptide bond between a highly conserved arginine pair in subunit I, one of which interacts with a propionate substitutent of the heme *a* through another hydrogen bond. In addition, the arginine pair is also hydrogen-bonded to a heme a_3 propionate and to the Mg ligand, D412. Previous studies have shown that the position of the α-peak of heme *a* is strongly influenced by interactions between heme *a* and Tyr-414 (*45*) and Arg-52 (*64*). Mutation of Arg-52 was observed to cause a 10 nm blue-shift of the heme *a* α-peak, while mutation of Tyr-414 causes it to shift 5 nm in opposite direction. It is possible that the mutation of His-260 produces some structural disturbance of Arg-52, accounting for the small shift of the α-peak in H260N (Figure 1).

In the Cu_A center, residue His-260 is a strong ligand of the lower of the two copper ions, along with Glu-254; the latter residue interacts less strongly with the same copper via its main-chain carbonyl and with the Mg ion via its carboxyl (*4*). The mutation of residue His-260 may thus alter the position of Glu-254 and other nearby residues, affecting the structure of the Mg/Mn center. But as in the case of M263L (the weaker ligand of the upper of the two copper ions), the heme a_3-Cu_B center in H260N is not disturbed, as shown from the FTIR and CO binding studies.

(ii) EPR Analysis of the Cu_A Center. Surprisingly, metal analyses show that there are still two copper atoms at the Cu_A centers in both H260N and M263L, even though their

EPR spectra are severely altered. In the high-field $g_\perp$ spectrum of M263L, the signal is resolved into a seven-line hyperfine pattern, a characteristic of a mixed valence dinuclear center. The electronic density on the dinuclear coppers on M263L increases as indicated by the increase of A_x^{Cu} from 28 G in wild-type to 36 G in the mutant (Table 2). The decrease of the intensity of the g_{II} region is attributed to multiple forms caused by greater strain induced by the mutation, perturbing the axial but not the Cu_2S_2 plane. However, it is difficult to estimate the electronic state of the Cu_A center in CcO solely based on the X-band spectrum (*1*), and therefore, multifrequency EPR spectra were recorded for M263L in this study. At X-, C-, and S-band frequencies, partial hyperfine splittings were resolved at the $g_\perp$ and g_{II} regions for M263L, and the *g*-values could be estimated from these hyperfine lines. The g-values were found to be invariant at the different frequencies if a seven-line hyperfine structure analysis was applied. A four-line hyperfine structure analysis for a decoupled or a mononuclear copper (as assumed with simulation of M227I, see below) resulted in different *g*-values at different frequencies. These studies strongly indicate that the Cu_A center in M263L is still a coupled dinuclear center. Studies on other mutant forms (*65*) of the soluble Cu_A domain of CcO from *Thermus thermophilus* (*10*), in which the equivalent methionine ligand was converted to glutamate (M160E) or glutamine (M160Q), also retain a coupled dinuclear center. In this case, stronger liganding at the methionine position is thought to be the effect of the Glu for Met substitution, resulting in more spin density on the coppers and a larger hyperfine coupling (*66*) as also observed here in M263L.

Perturbed X-band EPR spectra of Cu_A have been reported for M227I from *P. denitrificans* (*37*). The hyperfine pattern in the $g_\perp$ region in M227I is very similar to that found for M263L, but EPR simulation done on the X-band spectrum of M227I suggested that the altered Cu_A site in M227I is a type 1 copper with a decoupled configuration [Cu(1)−Cu(2)]. However, a more definitive method to determine whether the site is a mixed valence or a type 1 copper site is to measure the *g*-values as the microwave frequency is varied (Table 3) as discussed above. Since the two mutants of the methionine ligand have similar redox properties (see below) and spectral characteristics, it appears likely that both retain a coupled configuration of the Cu_A center, though altered compared to wild-type. In the case of H260N, further analysis will be required to determine if the two coppers are interacting.

Functional Effects of H260N and M263L. (i) Redox Potential Changes. Cu_A is the initial electron acceptor from cytochrome *c* (*13*, *67*). The redox potential of bovine cytochrome *c* is 260 mV in solution and lower when bound to CcO (*68*). The redox potential for Cu_A was found to be 260 mV in *P. denitrificans* oxidase (*37*), and in bovine oxidase, values of 250 mV and 360 mV were reported for Cu_A and heme *a*, respectively (*69*, *70*). Although the redox potentials for Cu_A and heme *a* in *R. sphaeroides* CcO have not yet been reported, the value for Cu_A is likely similar to that of bovine and *P. denitrificans* oxidases. However, the redox potential of heme *a* in the bacterial oxidases may be different from bovine oxidase, since their optical and EPR spectra are different. In *R. sphaeroides* CcO, the redox potential difference between heme *a* and Cu_A calculated from the rapid kinetics assay is about +50 mV ($\Delta E^\circ = E_a - E_{CuA}$; see the following paper in this issue) compared to ∼+100 mV in bovine (*14*). Assuming 250 mV for the redox potential of Cu_A in both oxidases, this suggests that the redox potential of heme *a* is about 300 mV (rather than 360 mV as for bovine).

In M263L, an altered redox potential of Cu_A is calculated from the rapid kinetics assay in the following study in the this issue. The redox difference between heme *a* and Cu_A ($\Delta E^\circ = E_a - E_{CuA}$) is about −72 mV, suggesting that the redox potential of the Cu_A site in M263L is about 120 mV more positive than that of the native Cu_A site; this is in good agreement with the result from the direct redox titration assay done on M227I from *P. denitrificans*, giving a midpoint potential of the altered Cu_A site about 100 mV higher than in the wild-type (*38*). The similar redox potentials observed for both M227I and M263L, in addition to their similar X-band EPR spectra, suggest that the altered Cu_A sites in the two mutants have similar electronic structure. The redox potential change, along with an expected change in reorganization energy, can account for the slower heme *a* reduction rate observed, as also concluded for the M227I mutant in *P. denitrificans* (*38*).

In the oxidation of fully reduced CcO, the fourth electron, originally in the Cu_A site, is required to convert the "ferryl" (or F) intermediate to the "oxidized" (or O) form. In M263L, the increase of the redox potential of Cu_A severely slows the electron-transfer rate from Cu_A to heme *a*, and alters the equilibrium between them. As a result, the conversion of the F intermediate to the O intermediate is slowed (*62*). The accumulation of intermediate F was also observed in M227I in *P. denitrificans* (*38*).

The slow reduction of heme a_3 in M263L is apparently not due to direct alteration of the heme a_3 (or Cu_B) center as suggested in the study of *P. denitrificans* (*37*) since FTIR and visible spectra indicate it is in a native configuration. It appears that the equilibrium favors Cu_A over heme a_3 reduction due to the 120 mV more positive redox potential of the Cu_A.

The situation in H260N is more complicated than in M263L. The redox potential difference between heme a and CuA is about −41 mV compared to +47 mV for wild-type, as estimated from the equilibrium in the rapid kinetics assay (see the following paper in this issue). As in the case of M263L, inhibition of electron transfer from Cu_A to heme *a* would be expected, due to the lower driving force and likely increase in reorganization energy, and is observed. However, heme *a* is also altered spectrally to a small extent, possibly having a higher positive redox potential as well, while the intrinsic electron-transfer rates (see the following paper in this issue) are far slower than for the M263L mutant. An even greater change in reorganization energy may be involved, but to account for the size of the rate change (∼1000-fold), an effect of this residue on a proposed hydrogen-bonded electron-transfer pathway must also be considered.

(ii) Proton Pumping. Besides being an initial electron acceptor, Cu_A was originally proposed to be involved in proton pumping (*71*). Current arguments against this model are based on the fact that quinol oxidases, which are homologous to CcO but do not have Cu_A centers, can still

pump protons (*72*). However, the quinol oxidases could conceivably use a different pumping mechanism, making this evidence not completely conclusive. In this study, both H260N and M263L have a significantly distorted Cu_A center, but retain proton pumping activity. The retention of proton pumping activity in these Cu_A mutants shows that the native structure of the Cu_A center is not required for proton pumping and adds strength to the conclusion that this center is not directly involved in the pumping mechanism.

SUPPORTING INFORMATION AVAILABLE

The deletion and the complementation of the *coxII*/*III* operon in *Rhodobacter sphaeroides* to create strain YZ200 is described in detail. This material is available free of charge via the Internet at http://pubs.acs.org.

REFERENCES

1. Beinert, H. (1997) *Eur. J. Biochem. 245*, 521−532.
2. Beinert, H., Griffiths, D., E, Wharton, D. C., and Sands, R. H. (1962) *J. Biol. Chem. 237*, 2337−2345.
3. Kroneck, P. M. H., Antholine, W. A., Riester, J., and Zumft, W. G. (1989) *FEBS Lett. 248*, 212−213.
4. Tsukihara, T., Aoyama, H., Yamashita, E., Tomizaki, T., Yamaguchi, H., Shinzawa-itoh, K., Nakashima, R., Yaono, R., and Yoshikawa, S. (1995) *Science 269*, 1069−1074.
5. Tsukihara, T., Aoyama, H., Yamashita, E., Tomizaki, T., Yamaguchi, H., Shinzawa-Itoh, K., Nakashima, R., Yaono, R., and Yoshikawa, S. (1996) *Science 272*, 1136−1144.
6. Iwata, S., Ostermeier, C., Ludwig, B., and Michel, H. (1995) *Nature 376*, 660−669.
7. Iwata, S., Saynovits, M., Link, T. A., and Michel, H. (1996) *Structure 4*, 567−579.
8. Yoshikawa, S., Shinzawa-Itoh, K., Nakashima, R., Yaono, R., Yamashita, E., Inoue, N., Yao, M., Fei, M. J., Libeu, C. P., Mizushima, T., Yamaguchi, H., Tomizaki, T., and Tsukihara, T. (1998) *Science 280*, 1723−1729.
9. Wilmanns, M., Lappalainen, P., Kelly, M., Sauer-Eriksson, E., and Saraste, M. (1995) *Proc. Natl. Acad. Sci. U.S.A. 92*, 11955−11959.
10. Williams, P. A., Blackburn, N. J., Sanders, D., Bellamy, H., Stura, E. A., Fee, J. A., and McRee, D. E. (1999) *Nat. Struct. Biol. 6*, 509−516.
11. Blackburn, N. J., Ralle, M., Gomez, E., Hill, M. G., Pastuszyn, A., Sanders, D., and Fee, J. A. (1999) *Biochemistry 38*, 7075−7084.
12. Hill, B. C. (1991) *J. Biol. Chem. 266*, 2219−2226.
13. Pan, L.-P., Hazzard, J. T., Lin, J., Tollin, G., and Chan, S. I. (1991) *J. Am. Chem. Soc. 113*, 5908−5910.
14. Pan, L. P., Hibdon, S., Liu, R.-Q., Durham, B., and Millett, F. (1993) *Biochemistry 32*, 8492−8498.
15. Zaslavsky, D., Sadoski, R. C., Wang, K., Durham, B., Gennis, R. B., and Millett, F. (1998) *Biochemistry 37*, 14910−14916.
16. Marcus, R. A., and Sutin, N. (1985) *Biochim. Biophys. Acta 811*, 265−322.
17. Farrar, J. A., Neese, F., Lappalainen, P., Kroneck, P. M. H., Saraste, M., Zumft, W. G., and Thomson, A. J. (1996) *J. Am. Chem. Soc. 118*, 11501−11514.
18. Gamelin, D. R., Randall, D. W., Hay, M. T., Houser, R. P., Mulder, T. C., Canters, G. W., de Vries, S., Tolman, W. B., Lu, Y., and Solomon, E. I. (1998) *J. Am. Chem. Soc. 120*, 5246−5263.
19. Salgado, J., Warmerdam, G., Bubacco, L., and Canters, G. W. (1998) *Biochemistry 37*, 7373−7389.
20. Brzezinski, P. (1996) *Biochemistry 35*, 5612−5615.
21. Onuchic, J. N., Beratan, D. N., Winkler, J. R., and Gray, H. B. (1992) *Annu. Rev. Biophys. Biomol. Struct. 21*, 349−377.
22. Moser, C. C., Page, C. C., Farid, R., and Dutton, P. L. (1995) *J. Bioenerg. Biomembr. 27*, 263−274.
23. Ramirez, B. E., Malmstrom, B. G., Winkler, J. R., and Gray, H. B. (1995) *Proc. Natl. Acad. Sci. U.S.A. 92*, 11949−11951.
24. Zhen, Y., Hoganson, C. W., Babcock, G. T., and Ferguson-Miller, S. (1999) *J. Biol. Chem. 274*, 38032−38041.
25. Shapleigh, J. P., and Gennis, R. B. (1992) *Mol. Microbiol. 6*, 635−642.
26. Cao, J., Hosler, J., Shapleigh, J., Gennis, R., Revzin, A., and Ferguson-Miller, S. (1992) *J. Biol. Chem. 267*, 24273−24278.
27. Zhen, Y. (1998) in *Biochemistry*, Ph.D. Thesis. Michigan State University, East Lansing.
28. Ho, S. N., Hunt, H. D., Horton, R. M., Pullen, J. K., and Pease, L. R. (1989) *Gene 77*, 51−59.
29. Zhen, Y., Qian, J., Follmann, K., Hosler, J., Hayward, T., Nilsson, T., and Ferguson-Miller, S. (1998) *Protein Expression Purif. 13*, 326−336.
30. Hosler, J. P., Fetter, J., Tecklenburg, M. M. J., Espe, M., Lerma, C., and Ferguson-Miller, S. (1992) *J. Biol. Chem. 267*, 24264−24272.
31. Hosler, J. P., Espe, M. P., Zhen, Y., Babcock, G. T., and Ferguson-Miller, S. (1995) *Biochemistry 34*, 7586−7592.
32. Froncisz, W., and Hyde, J. S. (1982) *J. Magn. Reson. 47*, 515−521.
33. Antholine, W. E., Kastrau, D. H. W., Steffens, G. C. M., Buse, G., Zumft, W. G., and Kroneck, P. M. H. (1992) *Eur. J. Biochem. 209*, 875−881.
34. Fetter, J. R., Qian, J., Shapleigh, J., Thomas, J. W., García-Horsman, J. A., Schmidt, E., Hosler, J., Babcock, G. T., Gennis, R. B., and Ferguson-Miller, S. (1995) *Proc. Natl. Acad. Sci. U.S.A. 92*, 1604−1608.
35. Hiser, C., Mills, D. A., Schall, M., and Ferguson-Miller, S. (2001) *Biochemistry 40*, 1606−1615.
36. Speno, H., Taheri, M. R., Sieburth, D., and Martin, C. T. (1995) *J. Biol. Chem. 270*, 25363−25369.
37. Zickermann, V., Verkhovsky, M., Morgan, J., Wikström, M., Anemuller, S., Bill, E., Steffens, G. C., and Ludwig, B. (1995) *Eur. J. Biochem. 234*, 686−693.
38. Zickermann, V., Wittershagen, A., Kolbesen, B. O., and Ludwig, B. (1997) *Biochemistry 36*, 3232−3236.
39. Kelly, M., Lappalainen, P., Talbo, G., Haltia, T., van der Oost, J., and Saraste, M. (1993) *J. Biol. Chem. 268*, 16781−16787.
40. Farrar, J. A., Lappalainen, P., Zumft, W. G., Saraste, M., and Thomson, A. J. (1995) *Eur. J. Biochem. 232*, 294−303.
41. den Blaauwen, T., van de Kamp, M., and Canters, G. W. (1991) *J. Am. Chem. Soc. 113*, 5050−5052.
42. Depillis, G. D., Decatur, S. M., Barrick, D., and Boxer, S. G. (1994) *J. Am. Chem. Soc. 116*, 6981−6982.
43. Goldsmith, J. O., King, B., and Boxer, S. G. (1995) *Biochemistry 35*, 2421−2428.
44. Eglinton, D. G., Johnson, M. K., Thomson, A. J., Gooding, P. E., and Greenwood, C. (1980) *Biochem. J. 191*, 319−331.
45. Hosler, J. P., Ferguson-Miller, S., Calhoun, M. W., Thomas, J. W., Hill, J., Lemieux, L., Ma, J., Georgiou, C., Fetter, J., Shapleigh, J. P., Tecklenburg, M. M. J., Babcock, G. T., and Gennis, R. B. (1993) *J. Bioenerg. Biomembr. 25*, 121−136.
46. Shapleigh, J. P., Hill, J. J., Alben, J. O., and Gennis, R. B. (1992) *J. Bacteriol. 174*, 2338−2343.
47. Zickermann, V., Verkhovsky, M., Morgan, J., Wikstrom, M., Anemuller, S., Bill, E., Steffens, G. C., and Ludwig, B. (1995) *Eur. J. Biochem. 234*, 686−693.
48. Kroneck, P. M. H., Anotholine, W. E., Riester, J., and Zumft, W. G. (1988) *FEBS Lett. 242*, 70−74.
49. Wang, X., Berry, S. M., Xia, Y., and Lu, Y. (1999) *J. Am. Chem. Soc. 121*, 7449−7451.
50. Zhen, Y., Mills, D., Hoganson, C. W., Lucas, R. L., Shi, W., Babcock, G., and Ferguson-Miller, S. (1999) in *Frontiers of Cellular Bioenergetics: Molecular Biology, Biochemistry and Physiopathology* (Papa, S., Guerrieri, F., and Tager, J. M., Eds.) pp 157−178, Plenum Press, New York.
51. Tsudzuki, T., and Wilson, D. (1971) *Arch. Biochem. Biophys. 145*, 149−154.
52. Eglinton, D. G., Johnson, M. K., Thomson, A. J., Gooding, P. E., and Greenwood, C. (1980) *Biochem. J. 191*, 319−331.
53. Greenwood, C., Hill, B. C., Barber, D., Eglinton, D. G., and Thomson, A. J. (1983) *Biochem. J. 215*, 303−316.
54. Beinert, H., Shaw, R. W., Hansen, R. E., and Hartzell, C. R. (1980) *Biochim. Biophys. Acta 591*, 458−470.

55. Boelens, R., Wever, R., and Van Gelder, B. F. (1982) *Biochim. Biophys. Acta 682*, 264−272.
56. Powers, L., Blumberg, W. E., Chance, B., Barlow, C. H., Leigh, J. S. j., Smith, J., Yonetani, T., Vik, S., and Peisach, J. (1979) *Biochim. Biophys. Acta 546*, 520−538.
57. Hendler, R. W., Harmon, P. A., and Levin, I. W. (1994) *Biophys. J. 67*, 2493−2500.
58. Lappalainen, P., Aasa, R., Malmström, B. G., and Saraste, M. (1993) *J. Biol. Chem. 268*, 26416−26421.
59. Rich, P. R., Moody, A. J., and Ingledew, W. J. (1992) *FEBS lett. 305*, 171−173.
60. Einarsdottir, O., Georgiadis, K. E., and Dawes, T. D. (1992) *Biochem. Biophys. Res. Commun. 184*, 1035−1041.
61. Hill, B. C., and Peterson, J. (1998) *Arch. Biochem. Biophys. 350*, 273−282.
62. Karpefors, M., Adelroth, P., Zhen, Y., Ferguson-Miller, S., and Brzezinski, P. (1998) *Proc. Natl. Acad. Sci. U.S.A. 95*, 13606−11.
63. Ostermeier, C., Harrenga, A., Ermler, U., and Michel, H. (1997) *Proc. Natl. Acad. Sci. U.S.A. 94*, 10547−10553.
64. Kannt, A., Pfitzner, U., Ruitenberg, M., Hellwig, P., Ludwig, B., Mantele, W., Fendler, K., and Michel, H. (1999) *J. Biol. Chem. 274*, 37974−37981.
65. Slutter, C., Gromov, I., Richards, J., Pecht, I., and Goldfarb, D. (1999) *J. Am. Chem. Soc. 121*, 5077−5078.
66. Slutter, C., Gromov, I., Epel, B., Pecht, I., Richards, J., and Goldfarb, D. (2001) *J. Am. Chem. Soc. 123*, 5325−5336.
67. Hill, B. C. (1993) *J. Bioenerg. Biomembr. 25*, 115−120.
68. Schroedl, N. A., and Hartzell, C. R. (1977) *Biochemistry 16*, 4961−4965.
69. Wilson, D. F., Linsay, G., and Brocklehurst, E. S. (1972) *Biochim. Biophys. Acta 256*, 277−286.
70. Wilson, D. F., Erecinska, M., and Owen, C. S. (1976) *Arch. Biochem. Biophys. 175*, 160−72.
71. Chan, S. I., and Li, P. M. (1990) *Biochemistry 29*, 1−12.
72. Puustinen, A., Finel, M., Virkki, M., and Wikström, M. (1989) *FEBS Lett. 249*, 163−167.

BI0114628